INTERNATIONAL JOURNAL OF INTEGRATED ENGINEERING
ISSN: 2229-838X e-ISSN: 2600-7916

IJIE

Vol. 16 No. 8 (2024) 20-30
https://publisher.uthm.edu.my/ojs/index.php/ijie

Stagnation-point Flow of a Hybrid Nanofluid Over an Exponentially Stretching Sheet with Zero Mass Flux Boundary Condition

N. A. Halim[1]*, N. S. A. Affrizal[1], N. I. M. Amin[1]

[1] *School of Mathematical Sciences, College of Computing, Informatics and Mathematics, Universiti Teknologi MARA, 40450 Shah Alam, Selangor, MALAYSIA*

*Corresponding Author: nadhirahhalim@uitm.edu.my
DOI: https://doi.org/10.30880/ijie.2024.16.08.003

Article Info

Received: 7 June 2024
Accepted: 12 October 2024
Available online: 21 November 2024

Keywords

Hybrid nanofluid, stagnation-point flow, zero mass flux

Abstract

Research on boundary layer flow and heat transfer characteristics of hybrid nanofluid over exponential stretching surface using the modified Buongiorno nanofluid model (MBNM) with zero mass flux is still lacking. The model takes into consideration the effect of Brownian motion and thermophoresis as well as the effective properties of a hybrid nanofluid. The imposed zero normal flux condition assumes that the nanoparticle volume fraction on the surface is controlled passively via temperature gradient. The governing partial differential equations (PDEs) are transformed into ordinary differential equations (ODEs) using appropriate similarity variables before being solved numerically using bvp4c in MATLAB. Obtained results are presented in graphical and tabular form. An 8.82% increment was observed in the values of Nusselt numbers of hybrid nanofluid as compared to base fluid. The stagnation parameter and nanoparticle volume fraction are important factors in improving the heat transfer rate of the fluid. The Nusselt number is an increasing function of both parameters. Meanwhile, the Brownian motion parameter has a negligible effect on the heat transfer rate.

1. Introduction

Many manufacturing processes revolve around the manipulation and treatment of heat and mass transfer of fluid flowing over a continuously moving or stretching surface. The thermoforming method requires stretching the heated plastic before cooling it to retain the desired shapes. In sheet glass production, molten glass is poured onto the conveyor and then cooled and solidified into a flat sheet. Similarly, the production of paper, polymer sheets, hot rolling, and wire drawing all involve the kinematics of stretching and simultaneous heating or cooling. These are important aspects of the manufacturing processes as they can affect the desired quality of the final products. As such, it is of equal importance that studies are made to examine the heat transfer rate and characteristics of the fluid flow near a stretching surface.

[1] head started the investigation in 1970 by considering a steady boundary layer flow of a viscous incompressible fluid due to a linearly stretching plate. The research has since then taken off with various aspects of such flow taken into consideration by investigators around the world. However, many studies assumed a linear relationship with the distance from the fixed origin, though in practicality, it may not necessarily be linear. [2] seem to be the first to consider the flow within the boundary layer caused by a surface undergoing exponential stretching in which they discussed the similarity solution involving an exponential dependence on the similarity variable. In addition to the expansive surface, the heat transfer fluid itself assumes a crucial role in the entirety of the industrial process. In recent years, hybrid nanofluid has become a credible heat transfer fluid that can improve

thermal efficiency. It is an upgraded version of nanofluids, in which nanosized solid particles made of metals, metal oxides, or carbon are dispersed in a base fluid of water, oil, or ethylene glycol. In the case of hybrid, two types of nanoparticles are dispersed instead of one.

Despite gaining interest from the researchers, flow analysis of hybrid nanofluid over an exponentially stretching surface is still relatively low as compared to the linearly stretching surface. [3] examine the hybrid nanoparticle effects on the fluid flow and heat transfer induced by an exponentially stretching/shrinking surface while considering the magnetohydrodynamic (MHD) and radiation effects. The findings indicate that maintaining sufficient suction strength is essential to sustain the flow over a shrinking sheet, and increasing radiation leads to a decrease in the rate of heat transfer. Other available works of literature on this exponential surface flow include ones by [4] that investigated the effect of heat generation, [5] who studied the mixed convection flow with Joule heating factor, [6] that investigated the stagnation point flow with buoyancy effects, while [7] includes MHD stagnation point flow with viscous dissipation in their study. Recently, [8] assessed the influence of TiO2-Ag/water on the flow with the effect of radiation and slip conditions and [9] addressed a natural stagnation bioconvection flow of a hybrid nanofluid containing gyrotactic microorganisms. The results in all the above literature agree on the existence of dual solutions for shrinking surfaces.

It is worth mentioning, that the two most used nanofluid mathematical models are those proposed by [10] and [11]. The Buongiorno model took into consideration the effect of Brownian motion and thermophoresis while the Tiwari-Das model considered the solid volume fractions of the nanoparticles. All the abovementioned literature is based on the Tiwari-Das model and studies on hybrid nanofluid using the Buongiorno model are still extremely limited. Some available literature includes one by [12] which investigates the impact of nanoparticle migration on hybrid nanofluid with natural convection. They examined an enclosure featuring sinusoidal wavy walls, with insulated upper and bottom walls. Their findings indicate that elevating thermophoresis diffusion enhances the heat transfer rate. Simultaneously, an increase in Brownian diffusion results in a higher concentration of nanoparticles near the hot wall. [13] conducted a sensitivity analysis using the Response Surface Methodology (RSM) on the heat transfer rate of hybrid nanofluid flow over a wedge. They considered two distinct heat sources, a linear thermal heat source, and an exponential space-dependent heat source for their study. Their results indicate that both heat mechanisms contribute to enhancing the temperature profile, with the exponential space-related heat source exerting a predominant effect. Meanwhile, [14] made a comparative study of Ag-MgO/water and Fe3O4-CoFe2O4/EG-water hybrid nanofluid flow over a curved surface. A larger value of the curvature parameter is found to decrease the mass transfer rate of the fluid. [15] presented a theoretical investigation to improve the efficiency of a solar water pump by utilizing the benefits of hybrid nanofluids' thermal characteristics with a parabolic trough solar collector.

The majority of existing hybrid nanofluid Buongiorno-based models have assumed constant nanoparticle concentrations in the proximity of the surface. A more physically realistic condition, as suggested by [16], introduces the notion that nanoparticle volume fractions near the surface are passively controlled by temperature gradients, leading to zero mass flux at the boundary. This condition was applied by [17] in their exploration of the impact of Hall's current on the flow of hybrid nanofluid over a slender stretching sheet. In the same year, [18] studied the flow and heat transfer characteristics using both nanofluid and hybrid nanofluid along a permeable isothermal stretching/shrinking surface. They discovered two solution branches within a specific range of suction, stretching/shrinking parameters, and hybrid nanofluids parameters. More recently, [19] investigated a three-dimensional flow and heat transfer of bi-directional stretched nanofluid film exposed to exponential heat generation. The findings indicated that the Brownian motion and thermophoresis contribute to a rise in the flow temperature, potentially influencing the nanoparticle concentration field as well.

Meanwhile, stagnation point flow can be used in various industrial processes where controlling the fluid behavior at a specific point is crucial. By controlling the point of impact, it can affect the surrounding pressure and fluid velocity which are used to analyze lift and drag forces in aerodynamics and heat transfer efficiency in cooling and heating systems, among others. [20] investigated the stagnation-point flow towards a stretching sheet and found that the resulting boundary layer depends on the ratio of the frictionless potential flow about the stagnation point to that of the velocity of the stretching surface. Thus, the present study aims to investigate the stagnation point flow of a hybrid nanofluid over an exponential stretching sheet with zero mass flux boundary conditions using the Buongiorno model. To the best of the author's knowledge, research has yet to be done under this specific condition. Thus, it is imperative that a study is made to study the flow characteristics and its heat transfer rate near the boundary layer, hopefully, to offer and add new knowledge on the vast and complex world of fluid systems.

2. Mathematical Formulation

The model of a two-dimensional constant stagnation-point flow of a hybrid nanofluid across a stretching sheet is formulated based on a few assumptions. The x-axis is parallel to the sheet and the y-axis is perpendicular to it in a Cartesian coordinate system. It is assumed that the flow is constrained at $y > 0$. Additionally, the sheet's surface temperature is maintained at T_w while the mass flux at the wall is assumed to be zero. Furthermore, T_∞ and C_∞

denote the ambient fluid temperature and concentration respectively. Both the free stream velocity away from the surface as well as the stretching surface velocity are assumed to vary nonlinearly, which corresponds to $u = u_e(x) = ae^{x/L}$ and $u = u_w(x) = be^{x/L}$, respectively where a and b are positive constants and L is the characteristic length of the sheet. Under the above assumptions, the governing equations are as follows [18]:

$$\frac{\partial u}{\partial x}+\frac{\partial v}{\partial y}=0, \tag{1}$$

$$u\frac{\partial u}{\partial x}+v\frac{\partial u}{\partial y}=u_e\frac{du_e}{dx}+\frac{\mu_{hnf}}{\rho_{hnf}}\frac{\partial^2 u}{\partial y^2}, \tag{2}$$

$$u\frac{\partial T}{\partial x}+v\frac{\partial T}{\partial y}=\frac{k_{hnf}}{\left(\rho C_p\right)_{hnf}}\frac{\partial^2 T}{\partial y^2}+\tau\left[D_B\frac{\partial C}{\partial y}\frac{\partial T}{\partial y}+\frac{D_T}{T_\infty}\left(\frac{\partial T}{\partial y}\right)^2\right], \tag{3}$$

$$u\frac{\partial C}{\partial x}+v\frac{\partial C}{\partial y}=D_B\frac{\partial^2 C}{\partial y^2}+\frac{D_T}{T_\infty}\frac{\partial^2 T}{\partial y^2}. \tag{4}$$

where u and v denote the velocity components in the x, and y-directions, μ is the dynamic viscosity of fluids, ρ is the density of fluids, k is the thermal conductivity of fluids, T is the fluid temperature, C is the fluid concentration, ρC_p is the heat capacity of fluids, D_B is the Brownian diffusion coefficient, D_T is the thermophoretic diffusion coefficient and $\tau = (\rho C_p)_s/(\rho C_p)_f$ is the ratio between the effective heat capacity of the nanoparticle material and heat capacity of the fluid. The associated boundary conditions are given as [4], [16]:
At $y = 0$:

$$u = u_w(x) = be^{x/L},\quad v = 0,\quad T = T_w,\quad D_B\frac{\partial C}{\partial y}+\frac{D_T}{T_\infty}\frac{\partial T}{\partial y}=0 \tag{5}$$

As $y \to \infty$:

$$u \to u_e(x) = ae^{x/L},\quad T \to T_\infty,\quad C \to C_\infty \tag{6}$$

Note that $(\cdot)_{hnf}$ in the governing equations denote the hybrid nanofluids quantities and are defined as follows (see [18]):

$$\frac{\rho_{hnf}}{\rho_f}=\left(1-\varphi_2\right)\left[1-\varphi_1+\varphi_1\frac{\rho_{s_1}}{\rho_f}\right]+\varphi_2\frac{\rho_{s_2}}{\rho_f}, \tag{7a}$$

$$\frac{\mu_{hnf}}{\mu_f}=\frac{1}{\left(1-\varphi_1\right)^{2.5}\left(1-\varphi_2\right)^{2.5}}, \tag{7b}$$

$$\frac{k_{hnf}}{k_f}=\frac{k_{s_2}+2k_{bf}+2\varphi_2\left(k_{s_2}-k_f\right)}{k_{s_2}+2k_{bf}-\varphi_2\left(k_{s_2}-k_f\right)}\quad where\quad \frac{k_{bf}}{k_f}=\frac{k_{s_1}+2k_f+2\varphi_1\left(k_{s_1}-k_f\right)}{k_{s_1}+2k_f-\varphi_1\left(k_{s_1}-k_f\right)} \tag{7c}$$

$$\frac{\left(\rho C_p\right)_{hnf}}{\left(\rho C_p\right)_f}=\left(1-\varphi_2\right)\left[1-\varphi_1+\varphi_1\frac{\left(\rho C_p\right)_{s_1}}{\left(\rho C_p\right)_f}\right]+\varphi_2\frac{\left(\rho C_p\right)_{s_2}}{\left(\rho C_p\right)_f} \tag{7d}$$

In this case, the base fluid quantities are represented by $(\cdot)_f$, while $(\cdot)_{s1}$, $(\cdot)_{s2}$, and φ_1, φ_2, signify the quantities of hybrid nanoparticles and the volume fraction of nanoparticles in the hybrid nanofluid, respectively ($\varphi_1 = \varphi_2 = 0$ corresponds to a regular fluid). The hybrid nanofluid is assumed to be homogeneous, hence, neglecting any internal fluctuations of the particle density or flows.

The governing equations along with their boundary conditions as in Eq. (1) to Eq. (6) can be transformed into a dimensionless form by employing the subsequent similarity transformations:

$$\eta = \sqrt{\frac{b}{2\nu_f L}} e^{x/2L} y, \quad \psi = \sqrt{2b\nu_f L} e^{x/2L} f(\eta), \qquad \theta = \frac{T - T_\infty}{T_w - T_\infty}, \quad \phi = \frac{C - C_\infty}{C_\infty}. \tag{8}$$

Eq. (1) is automatically satisfied and Eq. (2) to Eq. (6) takes the following forms:

$$\alpha_2 f''' + \alpha_1 \left(f f'' - 2(f')^2 + 2r^2 \right) = 0 \tag{9}$$

$$\frac{\alpha_4}{\alpha_3 \,\mathrm{Pr}} \theta'' + f\theta' + Nb\theta'\phi' + Nt(\theta')^2 = 0 \tag{10}$$

$$\phi'' + Le\, f\phi' + \frac{Nt}{Nb}\theta'' = 0 \tag{11}$$

subject to

$$f(0) = 0, \quad f'(0) = 1, \quad \theta(0) = 1, \quad Nb\phi'(0) + Nt\theta'(0) = 0, \tag{12}$$

$$f'(\infty) \to r, \quad \theta(\infty) \to 0, \quad \phi(\infty) \to 0. \tag{13}$$

In this expression,

$$\alpha_1 = \frac{\rho_{hnf}}{\rho_f}, \quad \alpha_2 = \frac{\mu_{hnf}}{\mu_f}, \quad \alpha_3 = \frac{(\rho C_p)_{hnf}}{(\rho C_p)_f}, \quad \alpha_4 = \frac{k_{hnf}}{k_f}. \tag{14}$$

Furthermore, primes denote the differentiation with respect to η, $r = a/b$ is the stagnation parameter, $Pr = \nu_f/\alpha$ is the Prandtl number in which $\alpha = k/\rho C_p$ is the thermal diffusivity, $Nb = \tau D_B C_\infty/\nu_f$ is the Brownian motion parameter, $Nt = \tau D_T(T_w - T_\infty)/\nu_f T_\infty$ is the thermophoresis parameter, and $Le = \nu_f/D_B$ is the Lewis number. Expressions for the local skin friction coefficient Cf_x and the local Nusselt number (or heat transfer rate), Nu_x are given by:

$$Cf_x = \frac{\tau_w}{\rho_f u_w^{\,2}(x)}, \qquad Nu_x = \frac{q_w L}{k_f (T_w - T_\infty)}, \tag{15}$$

where τ_w is the plate shear stress and q_w is the plate heat flux respectively.

$$\tau_w = \mu_{hnf} \left(\frac{\partial u}{\partial y} \right)_{y=0}, \qquad q_w = -k_{hnf} \left(\frac{\partial T}{\partial y} \right)_{y=0} \tag{16}$$

The dimensionless forms of Eq. (15) are given by:

$$Cf_x (2\,\mathrm{Re}_x)^{1/2} = \alpha_2 f'', \qquad Nu_x (\mathrm{Re}_x/2)^{-1/2} = -\alpha_4 \theta'(0) \tag{17}$$

where $Re_x = u_w(x) \cdot L/\nu_f$ is the local Reynolds number based on the stretching velocity $u_w(x)$.

There are different types of nanoparticles available, and the size, shape, and material used to make them can affect the thermal conductivity of the fluids [22]. Another essential factor is to choose a suitable combination of nanoparticles to ensure stable suspension of hybrid nanofluid [7]. In this study, the base fluid is water and the nanoparticles for the hybrid nanofluids are alumina (Al_2O_3), and copper (Cu). Both Al_2O_3 and Cu have high thermal conductivity, allowing an efficient heat transfer process. The physical properties of the hybrid nanofluids are given in Table 1.

Int. Journal of Integrated Engineering Vol. 16 No. 8 (2024) p. 20-30

Table 1 *Thermophysical properties of the base fluid and nanoparticles [21]*

Physical Properties	Base Fluid	Nanoparticles	
	Water	Al_2O_3	Cu
$\rho(kg/m^3)$	997.1	3970	8933
$C_p(J/kg\,K)$	4180	765	385
$k(W/m\,K)$	0.6071	40	400

3. Method of Solution

The governing ordinary differential equations in Eq. (9) to Eq. (13) were rewritten into a system comprising of seven first-order ordinary differential equations (ODEs), outlined as follows:

$$\begin{aligned}
x_1' &= f' = x_2 \\
x_2' &= f'' = x_3 \\
x_3' &= f''' = \frac{\alpha_1}{\alpha_2}\left[2x_2^{\,2} - x_1x_3 - 2r^2\right] \\
x_4' &= \theta' = x_5 \\
x_5' &= \theta'' = -\frac{\alpha_3}{\alpha_4}\Pr\left[x_1x_5 + Nbx_5x_7 + Nt(x_5)^2\right] \\
x_6' &= \phi' = x_7 \\
x_7' &= \phi'' = -\left[Le\,x_1x_7 + \frac{Nt}{Nb}x_5'\right]
\end{aligned} \tag{18}$$

with the boundary conditions:

$$\begin{aligned}
&x_1(0) = 0, \quad x_2(0) = 1, \quad x_4(0) = 1, \quad Nbx_7(0) + Ntx_5(0) = 0 \\
&x_2(\infty) \to r, \quad x_4(\infty) \to 0, \quad x_6(\infty) \to 0
\end{aligned} \tag{19}$$

The system as in Eq. (18) along with boundary conditions of Eq. (19) were then solved using MATLAB's *bvp4c* function which is a finite difference code that incorporates a collocation formula with fourth-order accuracy. It was evaluated at 100 equally spaced points, starting with zeros as the initial guesses, and the relative tolerance was taken to be 1×10^{-8}. The parameter η_∞ was assigned a value of 20 to ensure the convergence of all numerical solutions towards their respective asymptotic values as dictated by the specified boundary conditions.

To ensure computational accuracy, the results were validated through comparison with solutions obtained from another solver, specifically *dsolve* by MAPLE. This command directly determines the numerical solutions for the ODE system for Eq. (9) to Eq. (13) without the necessity of rewriting it as first-order ODEs. For boundary value problems (BVP), the default approach involves a finite difference technique with Richardson extrapolation. The initial mesh was set to 100 with an absolute error of 1×10^{-8}. Table 2 lists the compared values of skin friction, $Cf_x(2Re_x)^{1/2}$ and Nusselt number, $Nu_x(Re_x/2)^{-1/2}$ for various stagnation parameter, r values. From the table, it is safe to say that the current results are correct and accurate.

Table 2 *Values of skin friction and Nusselt number for various values of stagnation parameter, r*

Stagnation parameter, r	$Cf_x(2\,\mathrm{Re}_x)^{1/2}$		$Nu_x(\mathrm{Re}_x/2)^{-1/2}$	
	MATLAB *bvp4c*	MAPLE *dsolve*	MATLAB *bvp4c*	MAPLE *dsolve*
0.2	2.23452	2.2345202	1.74719	1.7471924
0.5	1.64503	1.6450311	1.87028	1.8702002
1	0	4.4352E-19	2.09402	2.0940221
1.5	-2.28109	-2.2810896	2.30886	2.3088646
1.8	-3.90311	-3.9031063	2.43105	2.4310472

4. Results and Discussion

The influence of several flow parameters like stagnation parameter, r; Lewis number, Le, Brownian motion parameter, Nb, thermophoresis parameter, Nt, Prandtl number, Pr; and nanoparticle volume fraction, φ, were

investigated and the results are presented through graphs. The parameter values used in the analysis were $r = 0.2$, $Pr = 6.135$, $Nb = Nt = 0.5$, $Le = 1$, and $\varphi_1 = \varphi_2 = 0.1$. In this study, φ_1 and φ_2 represent the nanoparticle volume fraction of alumina and copper respectively. Note that, due to the zero-mass flux assumption, values of concentration near the surface overshoot and attain negative values which are physically undefined but can be translated as the nanoparticle flux at the surface is suppressed [23].

Fig. 1 illustrates the impacts of stagnation parameter $r = a/b$ on velocity, temperature, and concentration. This parameter represents the ratio between stream velocity and surface velocity. To comprehend the influence of the stagnation parameter on velocity, three distinct cases can be examined. When $r > 1$, the stream velocity surpasses the surface velocity, leading to a reduction in the thickness of the velocity boundary layer as r increases. Conversely, $r = 1$ indicates that stream velocity is equal to the surface velocity, hence no velocity boundary layer forms due to the absence of changes in the fluid velocity. However, when $r < 1$, surface velocity exceeds the stream velocity, resulting in an inverted boundary layer. This observation aligns with the findings presented in [20]. The thickness of the velocity boundary layer has a direct impact on the heat transfer rate process through convection. A thick velocity boundary layer means the heat transfer process between the solid surface and fluid is less efficient. This results in a higher temperature gradient, hence decreasing the temperature. Besides that, if assuming that the stream velocity, c is constant, higher values of r mean lower surface velocity. Thus, increasing r means lower velocity which causes both heat and mass transfer to be less efficient resulting in lower temperature and concentration.

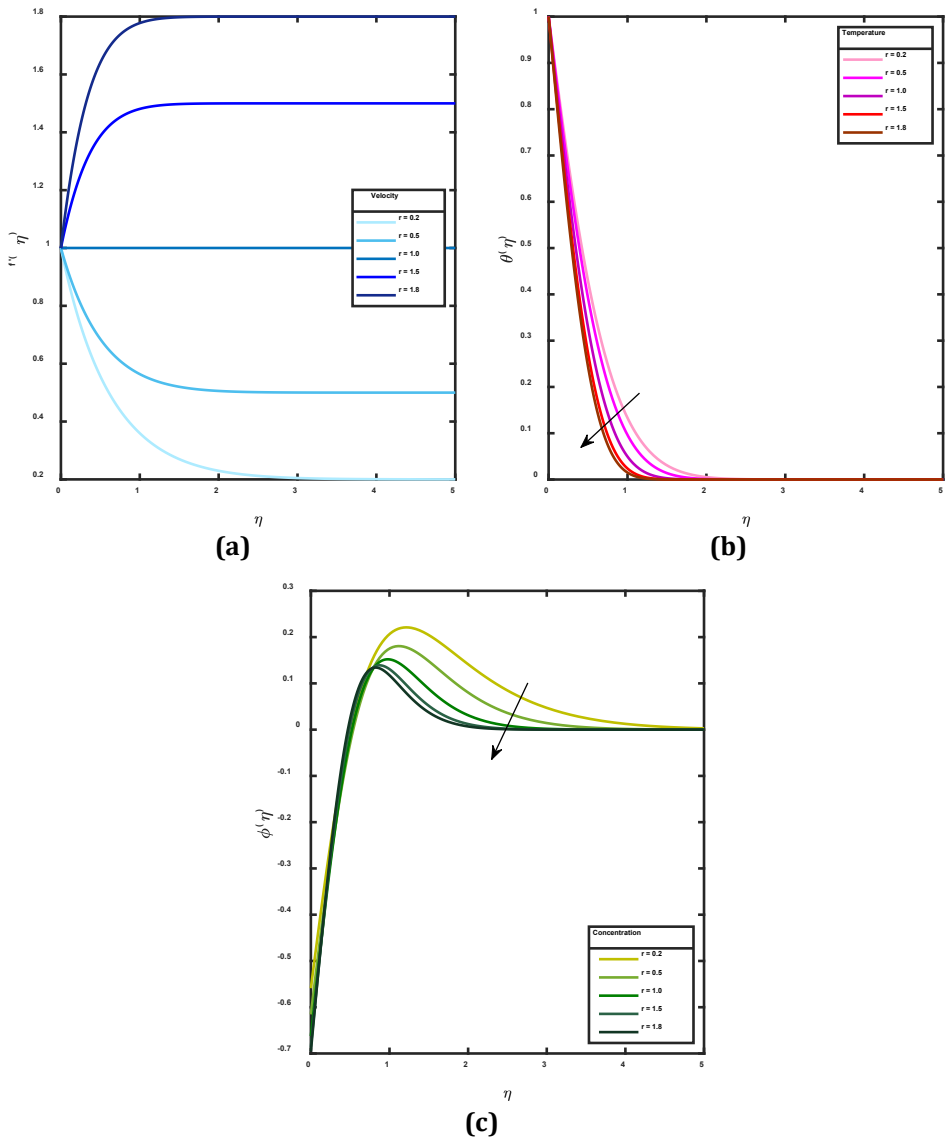

Fig. 1 *The effects of stagnation parameter, r towards (a) Velocity; (b) Temperature; and (c) Concentration profiles*

Fig. 2 shows the impact of the Lewis number on temperature and concentration. The Lewis number, denoted as *Le*, represents the ratio of thermal diffusivity to mass diffusivity. It is observed that as the Lewis number

Int. Journal of Integrated Engineering Vol. 16 No. 8 (2024) p. 20-30

increases, there is a corresponding increase in temperature. When $Le > 1$ thermal diffusivity is faster than mass diffusivity. Consequently, heat transfer transpires more swiftly, resulting in an elevation in temperature. It also shows that near the surface, the concentration increases as Le increases. When mass diffusivity decreases the concentration will be higher. However, moving away from the surface, the pattern reverses, and concentration starts to decrease. This shift could be attributed to other contributing factors that outweigh the influence of *Le*, thereby impacting fluid concentration.

Brownian motion refers to the unpredictable motion of particles suspended in a fluid, which results from collisions with neighboring molecules. The extent to which these particles disperse is quantified by the diffusion coefficient**.** Fig. 3 depicts the effects of the Brownian motion parameter, *Nb* on both temperature and concentration. It shows that when *Nb* increases, the temperature remains unchanged. This indicates that the heat resulting from the collisions is too small to make any significant changes in the fluid temperature. However, the concentration decreases as *Nb* increases. When there is more random particle movement, there is a higher chance of collision which increases the distance between the particles, resulting in lower concentration.

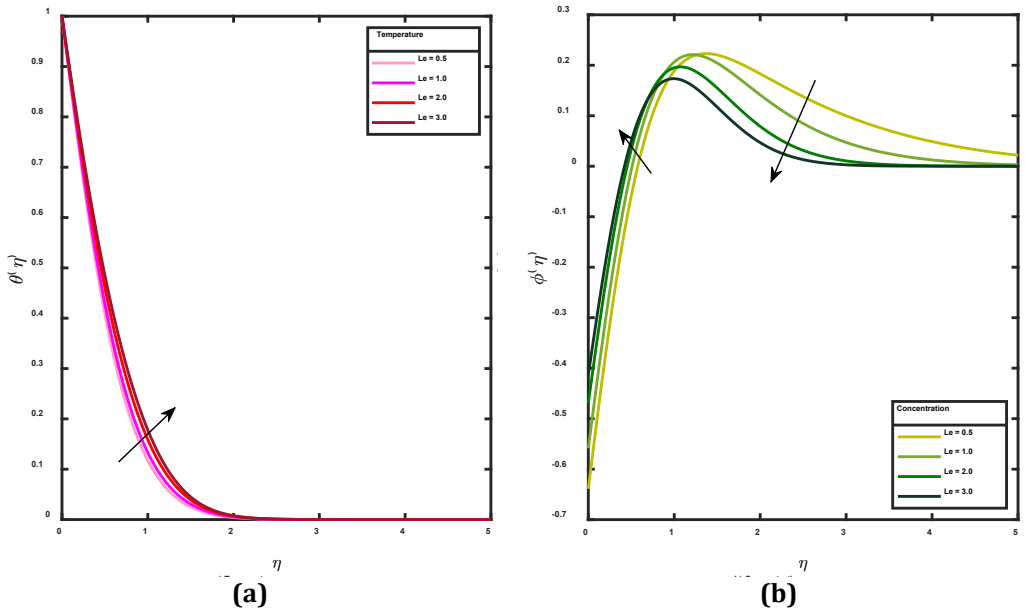

Fig. 2 *The effects of Lewis parameter, Le towards (a) temperature; and (b) concentration profiles*

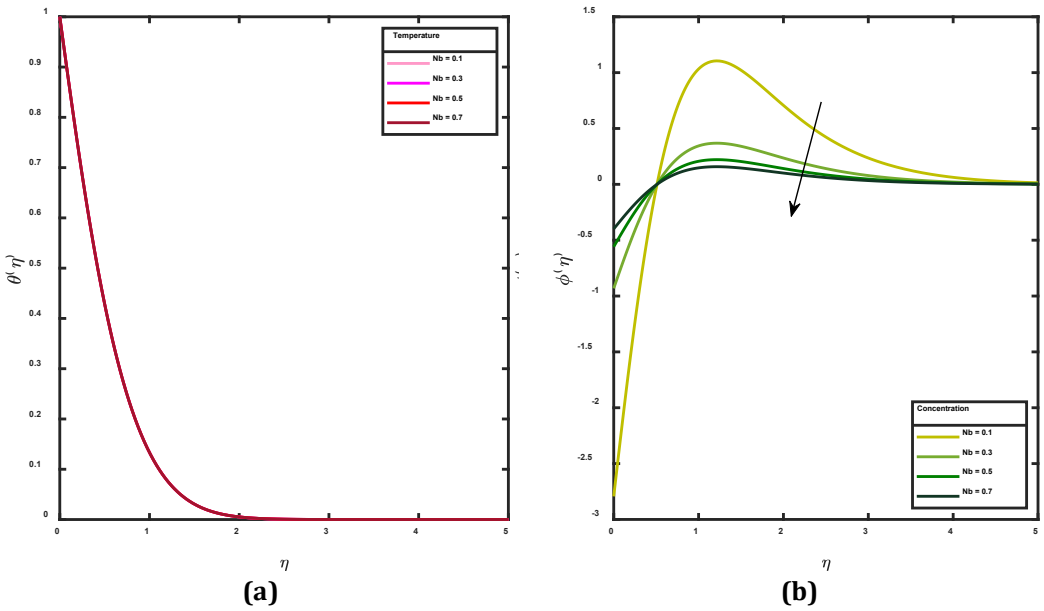

Fig. 3 *The effects of the Brownian motion parameter, Nb on (a) temperature; and (b) concentration profiles*

Meanwhile, thermophoresis describes the mass diffusion phenomenon due to temperature differences. As such, the thermophoresis parameter, *Nt* does not directly affect the fluid temperature and concentrations but

provides insights on how temperature gradient affects the particle motions. Fig. 4 shows that as *Nt* increases, both temperature and concentration increase. A higher thermophoresis parameter suggests a larger temperature gradient, hence higher temperature. And when there is a temperature gradient, particles tend to move from a high-temperature region to a lower-temperature region. The migration is what causes the changes in the fluid concentration. In this case, higher particle migration causes the fluid concentration to increase.

Fig. 5 shows the effects of changes in the nanoparticle volume fraction of Cu, φ_2. The fluid velocity decreases but temperature and concentration increase as the volume fraction of nanoparticles increases. As there are more nanoparticles in the mixture, the concentration is higher, and the fluid will be more viscous with higher resistance which results in decreasing velocity. With lower velocity, heat transfer is less effective causing the temperature to be higher. Note that $\varphi_2 = 0$ represents mono nanofluid and it is observed that m ono nanofluid has higher velocity, but lower temperature and concentration as compared to hybrid nanofluid.

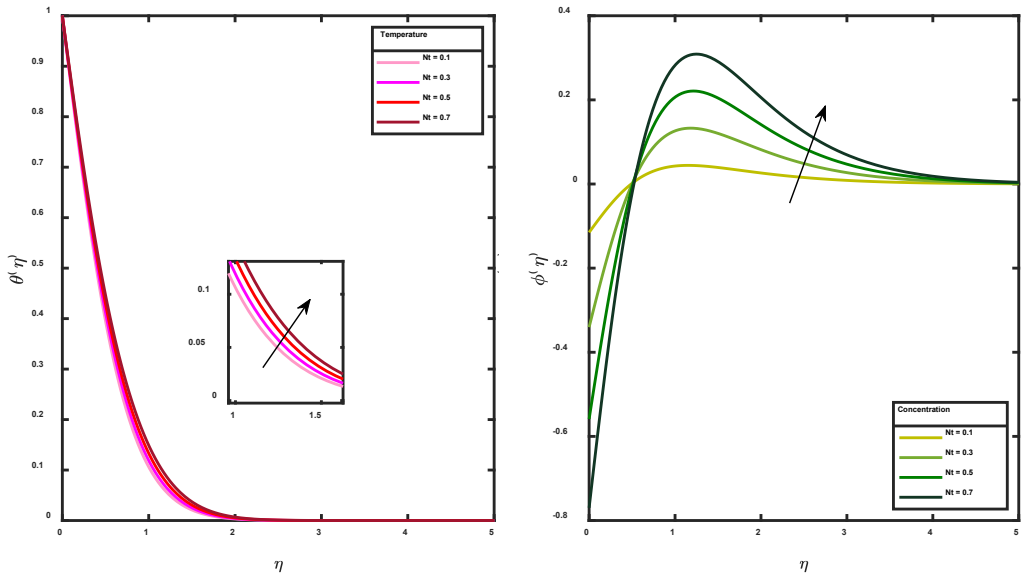

(a) **(b)**

Fig. 4 *The effects of thermophoresis parameter, Nt towards (a) temperature; and (b) concentration profiles*

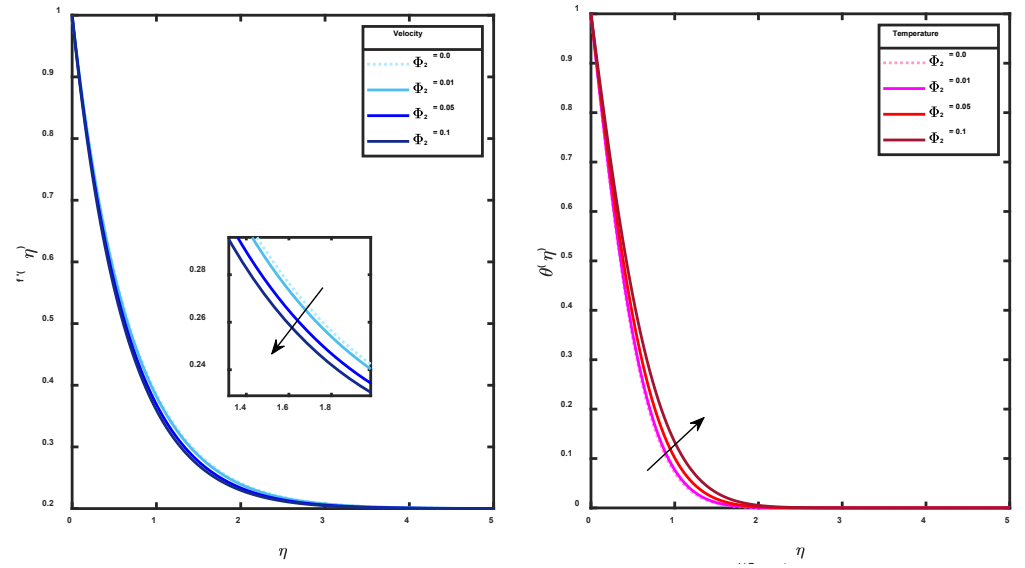

(a) **(b)**

Int. Journal of Integrated Engineering Vol. 16 No. 8 (2024) p. 20-30

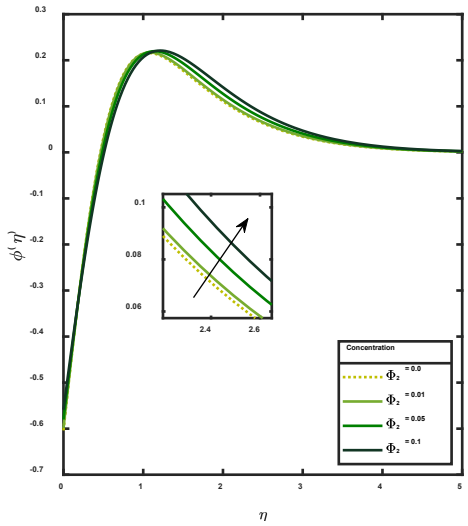

(c)

Fig. 5 *The effects of nanoparticle volume fraction, φ_2, on (a) velocity; (b) temperature; and (c) concentration profiles*

Values of reduced Nusselt number $Nu_x(Re_x/2)^{-1/2}$ and reduced skin friction $Cf_x(2Re_x)^{1/2}$ are shown in Table 3 along with parameter variations. The base fluid $(\varphi_1 = \varphi_2 = 0)$ exhibits the lowest skin friction, as anticipated due to the absence of additional nanoparticles that could contribute to friction between particles. Interestingly, the heat transfer rate of base fluid surpasses that of mono-nanofluids $(\varphi_2 = 0)$. This suggests the existence of a critical nanoparticle volume fraction that ensures an enhanced heat transfer rate for hybrid nanofluids. An 8.82% improvement in heat transfer rate was recorded when $\varphi_1 = \varphi_2 = 0.1$ as compared to the base fluid. It is also observed that skin friction is influenced solely by changes in parameter φ_2 and r, but with opposite reactions. It increases together with φ_2 but decreases as r increases. With increasing nanoparticle volume fraction, there is no doubt that there will be increasing resistance. As r represents the velocity ratio, increasing velocity will reduce the friction and become frictionless when there are no changes in velocity $(r = 1)$. The negative in skin friction simply represents changes in the direction of the friction. Simultaneously, the heat transfer rate rises in tandem with φ_2 and r, decreases with Le and Nt, and remains unaffected by Nb. From a practical standpoint, the direct controllability of both nanoparticle volume fraction and velocity ratio sets them apart as crucial factors in industrial processes compared to other parameters.

Table 3 *Values of $Cf_x(2Re_x)^{1/2}$ and $Nu_x(Re_x/2)^{-1/2}$ with parameter variation*

φ_1	φ_2	r	Le	Nb	Nt	$Cf_x(2Re_x)^{1/2}$	$Nu_x(Re_x/2)^{-1/2}$
0	0	0.2	1	0.5	0.5	1.19512	1.60557
0.1	0	0.2	1	0.5	0.5	1.55336	1.58129
	0.01					1.61874	1.59703
	0.05					1.88479	1.66179
	0.1					2.23452	1.74719
0.1	0.1	0.2	1	0.5	0.5	2.23452	1.74719
		0.5				1.64503	1.87028
		1.0				0	2.09402
		1.5				-2.28109	2.30886
		1.8				-3.90311	2.43105
0.1	0.1	0.2	0.5	0.5	0.5	2.23452	1.81603
			1			2.23452	1.74719
			2			2.23452	1.63456
			3			2.23452	1.54792
0.1	0.1	0.2	1	0.1		2.23452	1.74719
				0.3		2.23452	1.74719
				0.5		2.23452	1.74719
				0.7		2.23452	1.74719
0.1	0.1	0.2	1	0.5	0.1	2.23452	1.86520
					0.3	2.23452	1.80653
					0.5	2.23452	1.74719
					0.7	2.23452	1.68728

5. Conclusions and Recommendations

This study considered the problem of stagnation-point flow of a hybrid nanofluid over an exponentially stretching surface with zero mass flux condition using a modified Buongiorno nano-liquid model (MBNM). In practical applications, it is found that the surface velocity and nanoparticle volume fraction can be the key factor to control the desired heat transfer rate. The main findings of the study are:

- The stagnation parameter and nanoparticle volume fraction are important factors in improving the heat transfer rate of the fluid. The Nusselt number is an increasing function of both parameters.
- Increasing *Le* and *Nt* will increase the fluid temperature and reduce the heat transfer rate.
- Parameter *Nb* has no significant effect on either skin friction or the heat transfer rate.

For further research, this study can be extended to include other determining factors such as injection/suction, convective boundary condition, magnetohydrodynamic (MHD), and thermal radiation to name a few. It can also be applied to non-Newtonian fluids such as Maxwell, Carreau, and Jeffrey.

Acknowledgement

This research is financially supported by Universiti Teknologi MARA under research grant 600-RMC/GPM LPHD 5/3 (182/2021). A special appreciation to the School of Mathematical Sciences, College of Computing, Informatics, and Mathematics, Universiti Teknologi MARA for supporting the publication of this paper.

Conflict of Interest

Authors declare that there is no conflict of interest regarding the publication of the paper.

Author Contribution

The authors confirm contribution to the paper as follows: ***study conception and design:*** *N. A. Halim;* ***data collection:*** *N. A. Halim;* ***analysis and interpretation of results:*** *N. A. Halim, N. S. A. Affrizal, N. I. M. Amin;* ***draft manuscript preparation:*** *N. A. Halim, N. S. A. Affrizal, N. I. M. Amin. All authors reviewed the results and approved the final version of the manuscript.*

References

[1] Crane, L. J. (1970). Flow past a stretching plate. Zeitschrift für angewandte Mathematik und Physik ZAMP, 21, 645-647.
[2] Magyari, E., & Keller, B. (1999). Heat and mass transfer in the boundary layers on an exponentially stretching continuous surface. Journal of Physics D: Applied Physics, 32(5), 577.
[3] Waini, I., Ishak, A., & Pop, I. (2020). Hybrid nanofluid flow induced by an exponentially shrinking sheet. Chinese Journal of Physics, 68, 468-482.
[4] Wahid, N. S., Arifin, N. M., Khashi'ie, N. S., & Pop, I. (2020). Hybrid nanofluid slip flows over an exponentially stretching/shrinking permeable sheet with heat generation. Mathematics, 9, 30.
[5] Yashkun, U., Zaimi, K., Ishak, A., Pop, I., & Sidaoui, R. (2021). Hybrid nanofluid flows through an exponentially stretching/shrinking sheet with mixed convection and Joule heating. International Journal of Numerical Methods for Heat & Fluid Flow, 31, 1930-1950.
[6] Waini, I., Ishak, A., & Pop, I. (2021). Hybrid nanofluid flow towards a stagnation point on an exponentially stretching/shrinking vertical sheet with buoyancy effects. International Journal of Numerical Methods for Heat & Fluid Flow, 31, 216-235.
[7] Zainal, N. A., Nazar, R., Naganthran, K., & Pop, I. (2021). Viscous dissipation and MHD hybrid nanofluid flow towards an exponentially stretching/shrinking surface. Neural Computing and Applications, 1-11.
[8] Patel, V. K., Pandya, J. U., & Patel, M. R. (2023). Testing the influence of TiO2− Ag/water on hybrid nanofluid MHD flow with effect of radiation and slip conditions over exponentially stretching & shrinking sheets. Journal of Magnetism and Magnetic Materials, 572, 170591.
[9] Soid, S. K., Ab Talib, S. N. A., Norzawary, N. H. A., Isa, S. S. P. M., & Mohamed, M. K. A. (2023). Stagnation bioconvection flow of Titanium and Aluminium alloy nanofluid containing Gyrotactic Microorganisms over an exponentially vertical sheet. Journal of Advanced Research in Fluid Mechanics and Thermal Sciences, 107, 202-218.
[10] Buongiorno, J. (2006). Convective transport in nanofluids. ASME Journal of Heat and Mass Transfer 128, 240–250.
[11] Tiwari, R. K., & Das, M. K. (2007). Heat transfer augmentation in a two-sided lid-driven differentially heated square cavity utilizing nanofluids. International Journal of Heat and Mass Transfer, 50, 2002-2018.
[12] Goudarzi, S., Shekaramiz, M., Omidvar, A., Golab, E., Karimipour, A., & Karimipour, A. (2020). Nanoparticles migration due to thermophoresis and Brownian motion and its impact on Ag-MgO/Water hybrid nanofluid natural convection. Powder Technology, 375, 493-503.

[13] Mahanthesh, B., Shehzad, S. A., Mackolil, J., & Shashikumar, N. S. (2021). Heat transfer optimization of hybrid nanomaterial using modified Buongiorno model: A sensitivity analysis. International journal of heat and mass transfer, 171, 121081.
[14] Mishra, A., & Upreti, H. (2022). A comparative study of Ag–MgO/water and Fe3O4–CoFe2O4/EG–water hybrid nanofluid flow over a curved surface with chemical reaction using Buongiorno model. Partial Differential Equations in Applied Mathematics, 5, 100322.
[15] Shahzad, F., Jamshed, W., Eid, M. R., Safdar, R., Putri Mohamed Isa, S. S., El Din, S. M., ... & Iqbal, A. (2022). Thermal cooling efficacy of a solar water pump using Oldroyd-B (aluminum alloy-titanium alloy/engine oil) hybrid nanofluid by applying new version for the model of Buongiorno. Scientific Reports, 12, 19817.
[16] Kuznetsov, A. V., & Nield, D. A. (2013). The Cheng–Minkowycz problem for natural convective boundary layer flow in a porous medium saturated by a nanofluid: a revised model. International Journal of Heat and Mass Transfer, 65, 682-685.
[17] Das, K., Giri, S. S., & Kundu, P. K. (2021). Influence of Hall current effect on hybrid nanofluid flow over a slender stretching sheet with zero nanoparticle flux. Heat Transfer, 50, 7232-7250.
[18] Roşca, N. C., Roşca, A. V., Aly, E. H., & Pop, I. (2021). Flow and heat transfer past a stretching/shrinking sheet using a modified Buongiorno nanoliquid model. Mathematics, 9, 3047.
[19] Owhaib, W., & Al-Kouz, W. (2022). Three-dimensional numerical analysis of flow and heat transfer of bi-directional stretched nanofluid film exposed to an exponential heat generation using modified Buongiorno model. Scientific Reports, 12, 10060.
[20] Mahapatra, T. R., & Gupta, A. S. (2002). Heat transfer in stagnation-point flow towards a stretching sheet. Heat and Mass Transfer, 38, 517-521.
[21] Devi, S. S. U., & Devi, S. P. (2016). Numerical investigation of three-dimensional hybrid Cu-Al2O3/water nanofluid flow over a stretching sheet with effecting Lorentz force subject to Newtonian heating. Canadian Journal of Physics, 94(5), 490-496.
[22] Suresh, S., Venkitaraj, K., P., Selvakumar, P., & Chandrasekar, M. (2011). Synthesis of Al2O3-Cu/water hybrid nanofluids using two-step method and its thermos physical properties. Colloids and Surfaces A: Physicochemical and Engineering Aspects, 388(1-3), 41-48.
[23] Ishfaq, N., Khan, Z. H., Khan, W. A., & Culham, R. J. (2016). Estimation of boundary-layer flow of a nanofluid past a stretching sheet: A revised model. Journal of Hydrodynamics, 28, 596-602.